

Mutations of the GNAS1 Gene, Stromal Cell Dysfunction, and Osteomalacic Changes in Non-McCune-Albright Fibrous Dysplasia of Bone

P. BIANCO,¹ M. RIMINUCCI,¹ A. MAJOLAGBE,² S. A. KUZNETSOV,² M. T. COLLINS,²
M. H. MANKANI,² A. CORSI,¹ H. G. BONE,³ S. WIENTROUB,⁴ A. M. SPIEGEL,⁵
L. W. FISHER,² and P. GEHRON ROBEY²

ABSTRACT

Activating missense mutations of the GNAS1 gene, encoding the α subunit of the stimulatory G protein (Gs), have been identified in patients with the McCune-Albright syndrome (MAS; characterized by polyostotic fibrous dysplasia, café au lait skin pigmentation, and endocrine disorders). Because fibrous dysplasia (FD) of bone also commonly occurs outside of the context of typical MAS, we asked whether the same mutations could be identified routinely in non-MAS FD lesions. We analyzed a series of 8 randomly obtained, consecutive cases of non-MAS FD and identified R201 mutations in the GNAS1 gene in all of them by sequencing cDNA generated by amplification of genomic DNA using a standard primer set and by using a novel, highly sensitive method that uses a protein nucleic acid (PNA) primer to block amplification of the normal allele. Histologic findings were not distinguishable from those observed in MAS-related FD and included subtle changes in cell shape and collagen texture putatively ascribed to excess endogenous cyclic adenosine monophosphate (cAMP). Osteomalacic changes (unmineralized osteoid) were prominent in lesional FD bone. In an *in vivo* transplantation assay, stromal cells isolated from FD failed to recapitulate a normal ossicle; instead, they generated a miniature replica of fibrous dysplasia. These data provide evidence that occurrence of GNAS1 mutations, previously noted in individual cases of FD, is a common and perhaps constant finding in non-MAS FD. These findings support the view that FD, MAS, and nonskeletal isolated endocrine lesions associated with GNAS1 mutations represent a spectrum of phenotypic expressions (likely reflecting different patterns of somatic mosaicism) of the same basic disorder. We conclude that mechanisms underlying the development of the FD lesions, and hopefully mechanism-targeted therapeutic approaches to be developed, must also be the same in MAS and non-MAS FD. (J Bone Miner Res 2000;15:120–128)

Key words: fibrous dysplasia, McCune-Albright syndrome, mutation analysis, Gs α , GNAS1, PNA, transplantation, animal model

INTRODUCTION

ACTIVATING MISSENSE mutations of the GNAS1 gene have been previously identified in patients with the McCune-Albright syndrome (MAS), which is defined by

the triad of polyostotic fibrous dysplasia, skin pigmentation, and endocrine disorders.^(1–3) R201C and R201H mutations of the encoded α subunit of the stimulatory G protein (Gs) result in loss of guanosine triphosphatase activity, increased stimulation of adenyl cyclase, and constitutively elevated

¹Dipartimento di Medicina Sperimentale, Università dell'Aquila, L'Aquila, Italy.

²Craniofacial and Skeletal Diseases Branch, National Institute of Dental and Craniofacial Research, National Institutes of Health, Bethesda, Maryland, U.S.A.

³Michigan Bone and Mineral Clinic, St. John's Medical Center, Detroit, Michigan, U.S.A.

⁴Department of Pediatric Orthopedics, Dana Children's Hospital, Tel Aviv Medical Center, Sackler School of Medicine, Tel Aviv University, Tel Aviv, Israel.

⁵Metabolic Diseases Branch, National Institute of Diabetes, Digestive, and Kidney Diseases, National Institutes of Health, Bethesda, Maryland, U.S.A.

TABLE 1. SYNOPSIS OF CLINICAL DATA AND MUTATION ANALYSIS RESULTS

Patient no.	Sex	Age (years)	FD	Site of lesion	Specimen/Technique	Mutation
1*	F	10	Monostotic (craniofacial)	Right temporal bone	Frozen bone [†]	R201H
2	F	20	Polyostotic (contiguous craniofacial)	Maxilla	MCDS ¹	R201C
3	M	6	Polyostotic (contiguous craniofacial)	Cranium	MCDS [†]	R201C
4	M	12	Polyostotic (axial and appendicular)	Femur, pelvis	Paraffin section [†]	R201H
5	M	16	Monostotic (craniofacial)	Maxilla	Fresh bone [‡]	R201H
6	F	13	Polyostotic (craniofacial)	Frontal bones	MCDC [‡]	R201C
7	F	35	Polyostotic (contiguous craniofacial)	Nasal area	MCDC [‡]	R201C
8 [§]	M	18	Monostotic (appendicular)	Metacarpal	MCDC [‡]	R201H

*Previously reported, patient 3.¹⁹

MCDS, multiclonal colony-derived strain of bone marrow stromal cells.

[†]gDNA sequence of PCR amplification product as previously described.¹⁸

[‡]gDNA sequence of PCR amplification product using PNA primer to block amplification of normal allele (see Materials and Methods).

[§]Undecalcified, plastic embedded specimen available.

intracellular cyclic adenosine monophosphate (cAMP).⁽⁴⁻⁷⁾ Isolated endocrine lesions in non-MAS patients have been associated with the same kind of mutations as MAS.⁽⁸⁻¹²⁾ Although the complete MAS is relatively uncommon, fibrous dysplasia (FD) of bone not associated with either skin pigmentation or endocrine disturbances is a frequent, and usually serious, skeletal disorder. FD of bone typically is categorized as monostotic, polyostotic, and MAS-associated forms.⁽¹³⁾ Whether non-MAS FD represents a phenocopy of the GNAS1-mutation associated MAS or a more limited expression of the same genetic disorder has not been conclusively addressed. Individual reports have mentioned the occurrence of GNAS1 mutations in cases of non-MAS FD.^(14,15) Jaffe and Lichtenstein also suggested a common etiology to both isolated FD and MAS-associated FD.^(16,17) Because a common genetic substrate implies a common mechanism of lesion development and potentially common therapeutic approaches tailored onto that mechanism, the issue is more than a mere academic exercise.

We investigated the occurrence of GNAS1 mutation in a consecutive series of 8 non-MAS FD patients by sequencing cDNA generated by amplification of genomic DNA using both a standard primer set and a novel method that relies on the use of a PNA (protein nucleic acid) primer to block amplification of normal allele. This report shows the consistent occurrence of R201C or R201H Gs α mutation in all of them, along with evidence for a similar dysfunctional state in osteogenic/stromal cells.

MATERIALS AND METHODS

Patients

A summary of clinical data of patients in this series is given in Table 1. For all patients, x-ray and histologic data were available for review. Specimens were collected from patients under an institutionally approved protocol (97-DK-0055). None of the patients in this series exhibited overt endocrine disturbance (4 of the 8 had undergone extensive endocrine evaluation, including analysis of vitamin D metabolites) or skin hyperpigmentation; the presence of either

condition was a criterion for exclusion from the present analysis. Patients with FD who exhibited endocrine hyperfunction or macular pigmented skin lesions were excluded.

Marrow stromal cell cultures

Marrow stromal cell cultures were established as previously described,⁽¹⁸⁾ with fresh surgical specimens of bone lesions from patients who underwent corrective surgery under a National Institutes of Health (NIH) institutional review board-approved protocol (97-DK-0055) and with normal marrow from sex- and age-matched donors (94-D-0188). Cell suspensions were obtained by scraping bone containing marrow into nutrient medium that consisted of alpha modified minimum essential medium (α -MEM; Biofluids, Inc., Rockville, MD, U.S.A.) plus 20% fetal bovine serum (Life Technology, Grand Island, NY, U.S.A.), glutamine, penicillin, and streptomycin (Biofluids, Inc.). A single cell suspension prepared by serial passage through needles of decreasing diameter and a cell sieve (70 μ m; Falcon, Becton Dickinson, Lincoln Park, NJ, U.S.A.), were plated into 75-cm² flasks and incubated at 37°C in an atmosphere of 100% humidity and 5% CO₂.

DNA extraction

For all patients, mutation analysis was performed by sequencing of polymerase chain reaction (PCR)-amplified genomic DNA. For patient 1, DNA was extracted from a frozen bone sample obtained at the time of surgery, and for patient 5, from fresh bone, as described previously.⁽¹⁹⁾ For patients 2, 3, 6, 7, and 8, DNA was extracted from cell cultures of clonogenic adherent stromal cells established from fresh surgical samples as described previously.⁽¹⁸⁾ Three million to five million marrow stromal cells (second or third passage) were released from the culture dish with trypsin and pelleted; then, the genomic DNA was purified by using a kit (Purogene, Minneapolis, MN, U.S.A.) and a standard protocol. For patient 4, DNA was extracted from a paraffin-embedded sample of FD by using the QIAamp Tissue Kit (Qiagen, Valencia, CA, U.S.A.) according to the

manufacturer's instructions. A small section from a paraffin block (not more than 2.5 mg) was placed in a 2-ml centrifuge tube, and paraffin was extracted with 1.2 ml of xylene. The sample was centrifuged, the supernatant was removed, and the precipitate was washed with 1.2 ml of absolute ethanol (5–7 times). The resulting pellet was allowed to air dry before the addition of extraction buffer and proteinase K. The subsequent procedure for DNA purification has been described previously.⁽¹⁹⁾

Determination of Gs α mutation

PCR amplification of genomic DNA was performed by using two different methods. Extracted DNA was dissolved in water, and 200–500 ng of genomic DNA was amplified in a 100- μ l reaction by PCR. For cases in which the majority of the cells were mutant (either present in the sample or grown in culture; patients 1–4), the mutation could be determined by directly sequencing a ~340-bp (genomic) product spanning the mutation site as described previously.⁽¹⁸⁾ For the PCR reaction, we used Perkin Elmer (Foster City, CA, U.S.A.) reagents and 2.5 U of Ampli Taq Gold polymerase, and 1 μ g each of forward primer (5'-TGACTATGTGCC-GAGCGA-3') and reverse primer (5'-CCACGTCAAACATGCTGGTG-3'). Samples were heated to 94°C for 15 minutes to activate the polymerase, cycled 35 times (94°C for 60 s, 55°C for 30 s, 72°C for 60 s), and terminated for 7 minutes at 72°C. The PCR products were purified using the Promega Wizard PCR Preps DNA Purification System (Madison, WI, U.S.A.). The DNA was then sequenced using an internal (reverse) primer (5'-CCACGTCAAACATGCTGGTG-3') by using dRhodamine dye-terminator cycle sequencing with Ampli Taq and the Perkin Elmer Applied Biosystems 377 automated sequencer.

For cases in which the majority of the cells in culture were not mutant (patients 5–8), we used a peptide nucleic acid (PNA) whose binding site overlapped the forward oligonucleotide to suppress the amplification of the nonmutant sequence. For this procedure, we used Perkin Elmer reagents and 2.5 U of Ampli Taq Gold polymerase; 1 μ g each of forward oligonucleotide (5'-GTTTCAGGACCTGCTTCGC-3') and reverse oligonucleotide (5'-GCAAAGCCAAGAGCGTGAG-3'); and 2 μ g of PNA (amino-terminal 5'-CGCTGCCGTGTC carboxy-terminal-3'). The samples were heated to 94°C for 15 minutes, cycled 40 times (94°C for 30 s, 68°C for 60 s [to allow the PNA to bind specifically to any nonmutant allele and block the annealing of the forward oligonucleotide], 55°C for 30 s, and 72°C for 60 s), and terminated for 7 min at 72°C. The ~325-bp PCR products were purified and sequenced as described earlier.

For the PNA-inhibition experiments, a sample of genomic DNA from normal control samples (derived from multiclonal-derived strains of normal bone marrow stromal cells) was amplified to check for contamination of reagents with mutant sequences. In all cases, samples were not amplified; that is, no amplification product was generated.

In vivo transplantation assay

Transplants of multiclonal-derived stromal cell strains from FD lesions in immunocompromised mice (NIH-bg-nu-

xidBR [beige], Harlan Sprague Dawley, Indianapolis, IN, U.S.A.) were performed as described previously using stromal cells derived from patients 2 and 3 and normal age-matched donors.^(18,20,21) Briefly, after ex vivo expansion, stromal cells were attached to hydroxyapatite/tricalcium phosphate ceramic particles (Zimmer, Warsaw, IN, U.S.A.) and transplanted subcutaneously into immunocompromised mice. The particles were irregular in shape, with rough surfaces, and 0.5–1.0 mm in size; pores were 0.025–0.1 mm. Transplants were harvested at 6–8 weeks. All procedures were performed in accordance with National Institute of Dental and Craniofacial Research (NIDCR) guidelines for the use of animals in research (97–024).

Histology

All samples were fixed with either Bouin's solution or 4% phosphate-buffered formaldehyde (PBF) freshly made from paraformaldehyde and then decalcified with ethylenediaminetetraacetic acid (EDTA), as previously described.⁽²²⁾ Tissues and transplants were embedded in paraffin, then 5- μ sections were prepared and stained with hematoxylin and eosin (H&E). In some cases, PBF-fixed, nondecalcified samples were embedded in methyl methacrylate, and then von Kossa and methylene blue stains were applied. H&E sections from paraffin blocks were viewed under transmitted, fluorescent, or polarized light.

RESULTS

Patient characterization

We identified 3 patients with monostotic FD and 5 with polyostotic FD. Of 8 patients in this series, 6 had craniofacial FD lesions and 2 had involvement of the axial-appendicular skeleton with spared craniofacial bones. Craniofacial lesions were clearly monostotic (a single site of involvement of a single bone) in two cases. A single site spanning different contiguous bone (as determined by CT scans) was involved in 4 patients and was considered to be polyostotic.

Mutation analysis

Cultures of dissected fibrous dysplastic lesions often can result in adherent cell populations that are greatly enriched in the somatic Gs α mutation. Amplifying this region of the genomic DNA by PCR can be used in automated DNA sequencing and result in a signal that is sufficiently rich in the mutant allele to allow the investigator to clearly discern the mutation (Fig. 1A, patient 3). Microdissected lesions themselves may also be rich enough in mutant cells to give a clear indication of the mutation. Indeed, in one case (patient 4), the genomic DNA could be extracted in sufficient quantities from a microdissected paraffin block to allow the assignment of the mutation type (Table 1; sequence not shown).

A culture of highly enriched mutant cells results in the DNA being roughly half wild type and half mutant, and the sequencing signals of both can be clearly seen (Fig. 1A, patient 3). However, as the number of mutant cells decreases to <50%, the amount of the mutant allele becomes <25%,

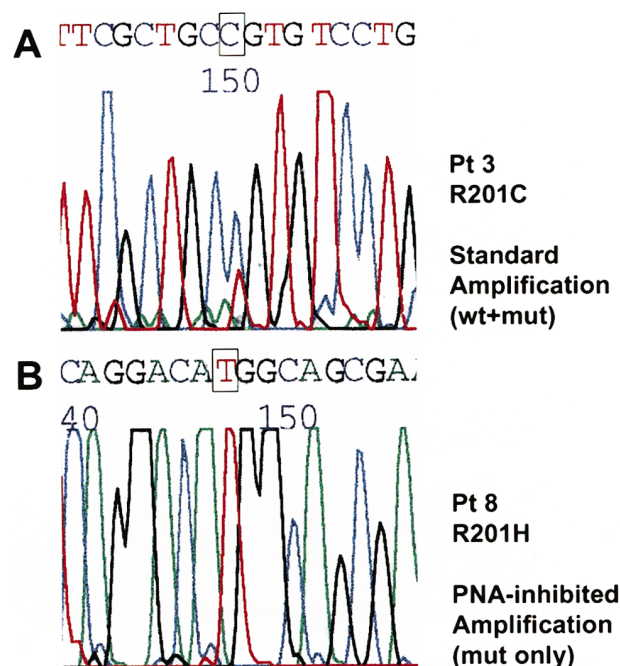


FIG. 1. Mutational analysis of genomic DNA isolated from FD tissue. (A) Forward sequencing reaction of genomic DNA from predominantly mutant cells of patient 3 (Pt 3) using standard PCR amplification and direct sequencing. The clear red T peak under wild-type C (boxed) was due to C-to-T mutation resulting in the R201C transition in the *Gsα* gene product. (B) PCR product for patient 8, when sequenced (in reverse, for technical reasons); a typical result for a R201H mutation. Notice that the mutation's T peak (boxed; reverse direction of the G-to-A mutation) is the only signal for the sequencing reaction. (C) PNA-inhibited approach to mutant sequence analysis. PNA (red) can bind to wild-type anti-sense sequences (top) but not to anti-sense strands of R201C (middle) or R201H (bottom) mutant alleles. Such a bound PNA cannot be extended by Taq polymerase (*). Without PNA blocking, the forward oligonucleotide can anneal to either mutated anti-sense strand and be extended (lowercase green) through the site of the mutation (#) by the Taq polymerase.



and it often becomes difficult to distinguish the mutant signal from background. To overcome this problem, a PNA was designed that specifically bound to the wild-type sequence, thereby blocking the annealing and extension of the overlapping forward primer. The properties of a properly designed PNA are that it binds strongly to the exact complementary sequence at temperatures above that of the competing true oligonucleotide (e.g., 68°C and 55°C); it does not significantly bind to a complementary sequence that is different by even one base; binding first at the higher

temperature, the PNA blocks the binding of the overlapping forward primer at the lower, annealing temperature; and the PNA, by its chemical nature, cannot be extended by the polymerase. However, the forward primer binds to the anti-sense strand of the mutant allele, because the PNA does not bind due to the single base-pair mismatch. Genomic DNA containing only a small percent of mutant allele results in a clear PCR band and a strong sequencing signal for the mutation (Fig. 1B, patient 8). Using the described PNA and oligo pairs, we have successfully sequenced genomic DNA

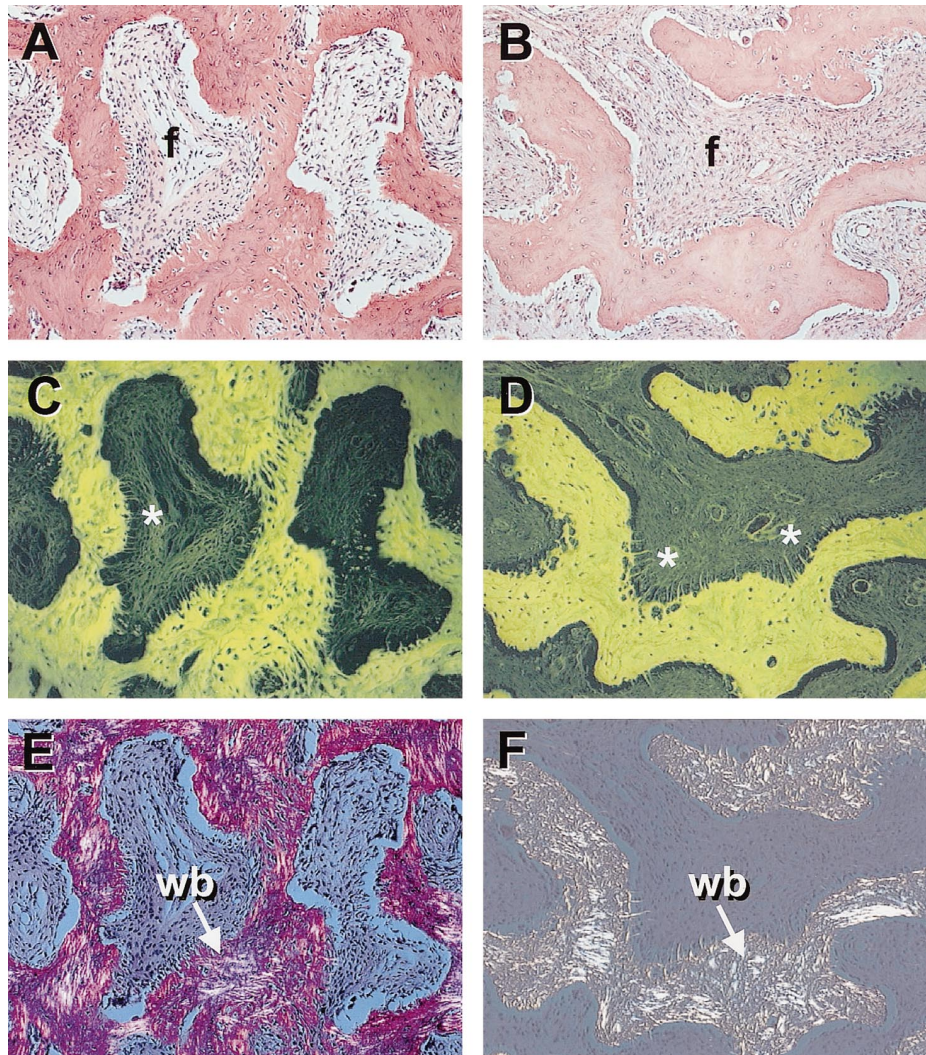


FIG. 2. Histology of FD tissue derived from patient 3 (A, C, and E) and from patient 8 (B, D, and F). (A and B) H&E staining shows replacement of normal bone and marrow with abnormal bone and fibrous tissue (f). (C and D) Same fields as in A and B, viewed with fluorescence microscopy to exploit the better resolution afforded by eosin-induced fluorescence. Note Sharpey fibers (perpendicular to the forming surface, as opposed to parallel) along the trabecular surfaces of FD bone (*). Complex systems of reversal or arrest lines, similar to Schmorl's mosaic, are apparent in C. (E and F) Same fields as in A and B, illuminated by polarized light. FD bone demonstrates a woven bone (wb) structure as opposed to the normal lamellar pattern.

from patients with R201C and R201H mutations. With our new technique, we have successfully determined the presence of a mutant allele in the equivalent of 1 cell in 50 (data not shown). Mutations outside of the Arg201 site, if any, would in this approach, result in no signal or only weak wild-type sequence.

Activating mutations of the *GNAS1* gene (R201H in 4 patients with either craniofacial or axial/appendicular disease, R201C in 4 patients with craniofacial disease) were demonstrated in all patients in this series (Table 1 and Fig. 1A, B). In all PNA-inhibited experiments, samples of genomic DNA derived from normal bone marrow stromal cells (multicolony-derived strains) failed to amplify, indicating that there was no contamination of samples with mutant sequences (data not shown).

Histologic features

In all patients, histology (Fig. 2, Fig. 3) and x-ray findings (not shown) were typical of FD. The classical "Chinese Writing" pattern⁽¹⁷⁾ (characterized by an abundance of fibrotic tissue surrounding scant and poorly formed trabeculae,

composed primarily of woven bone) was observed in the axial/appendicular lesions, whereas craniofacial samples were more osteosclerotic. The loss of hematopoiesis and adipogenesis, Sharpey fiber bone, Schmorl's mosaic-like patterns, and osteoblast cell-shape anomalies identified in MAS FD⁽¹⁹⁾ were all prominent in our series of non-MAS FD samples (Fig. 2, Fig. 3).

In addition to the features previously described, von Kossa staining of undecalcified plastic sections to clearly distinguish between mineralized and nonmineralized tissues revealed diffuse, thick osteoid seams along fibrodysplastic bone trabeculae (Fig. 3), indicating a mineralization defect in lesional bone.

Reproduction of FD by *in vivo* transplantation of populations containing mutated stromal cells

To further verify the malfunction of populations of FD stromal cells, we used an *in vivo* transplantation assay that we have previously developed for the assessment of stromal cell dysfunction in McCune-Albright syndrome.⁽¹⁸⁾ As expected, normal age-matched controls formed a complete

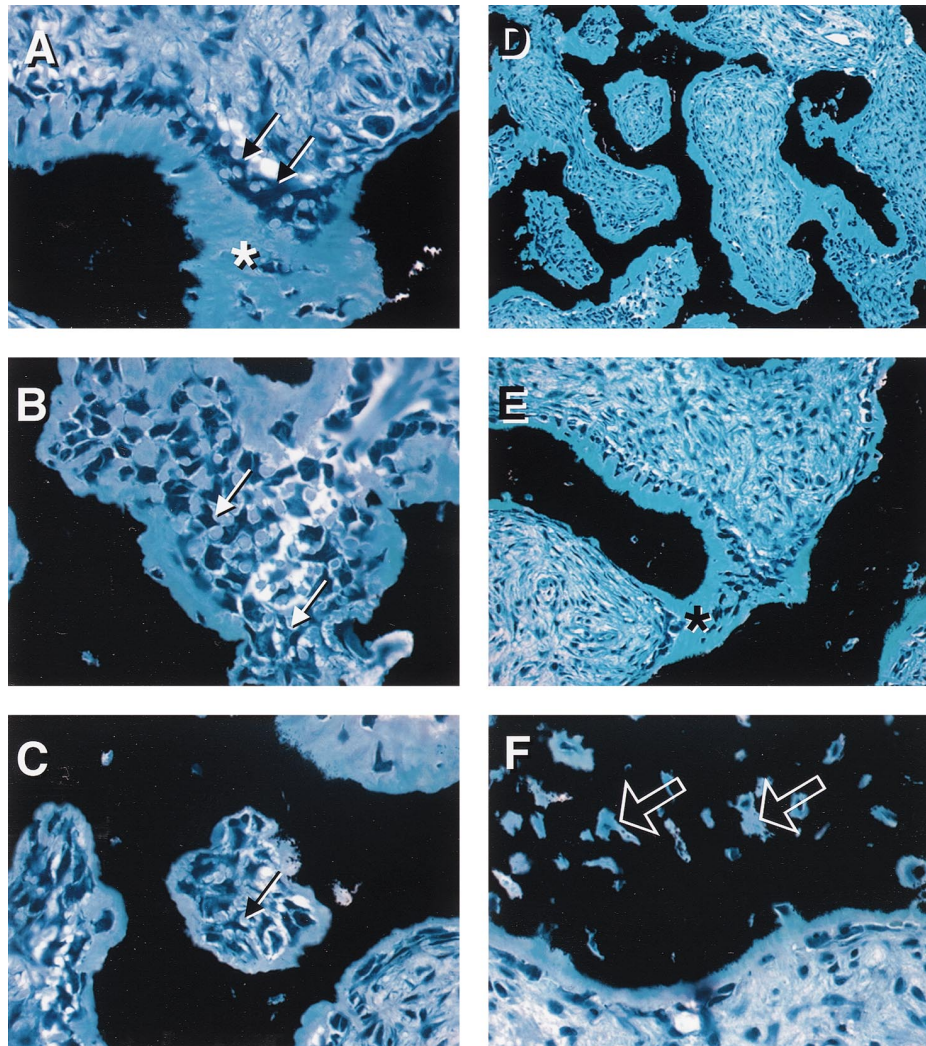


FIG. 3. Methyl methacrylate-embedded sections (patient 8) and von Kossa/methylene blue staining. Plastic embedded slides were stained with von Kossa stain and counterstained with methylene blue to distinguish between mineralized and unmineralized tissues and to facilitate resolution of cell shape details. Note the stellate/retracted shape of osteoblasts (A–C, arrows). Thick osteoid seams (D–F) (asterisks in A, E), indicating local osteomalacia within the FD lesion, are obvious in all panels. Osteocytic lacunae with unmineralized walls are also obvious in F (arrows).

bone/bone marrow organ in which lamellar bone, hematopoietic marrow, and adipocytes were both abundant and readily identified. In contrast, transplants of stromal cells derived from FD lesions, which contained cells carrying the activating mutation of the *GNAS1* gene, resulted in the formation of “fibrodysplastic” ossicles in which neither hematopoiesis nor adipogenesis developed (Fig. 4). The amount of bone formed was negligible in transplants from 1 patient, and slightly more abundant in those from the other. As determined by observation with polarized light microscopy, the bone tissue was woven in texture throughout in all transplants of cells derived from both patients, similar to what has been observed in patient material by scanning electron microscopy.⁽²³⁾

DISCUSSION

Previously, sporadic reports have described R201 mutations in individual FD patients not exhibiting a complete MAS.^(14,15) We investigated the potential occurrence of *GNAS1* mutations in the largest series of non-MAS FD

patients assembled to date. Our data, which shows the actual presence of mutation in all patients in a randomly acquired consecutive series, argues for FD being in many cases—if not always—a *Gsα* disease. We believe that there are important implications to these data, both conceptually and from an applicative point of view. Conceptually, the occurrence of *GNAS1* mutations in single skeletal lesions supports the view that variable expressions of the same genetic defect may arise as a consequence of different patterns of somatic mosaicism.^(5,24) Activating *GNAS1* mutations are thought to be lethal even in the heterozygotic state and to survive only if occurring postzygotically, thus leading to a somatic mosaic state.⁽²⁵⁾ It has been postulated that the precise postzygotic timing of the mutational “hit” would result in more or less widespread distribution of the progeny of the original mutated cell.^(5,24)

Furthermore, the number and distribution of the mutated cells may vary across postnatal tissues as a result of differential survival of the mutated cells during development. There is now substantial evidence for the occurrence of *GNAS1* mutations in isolated skeletal lesions (monostotic

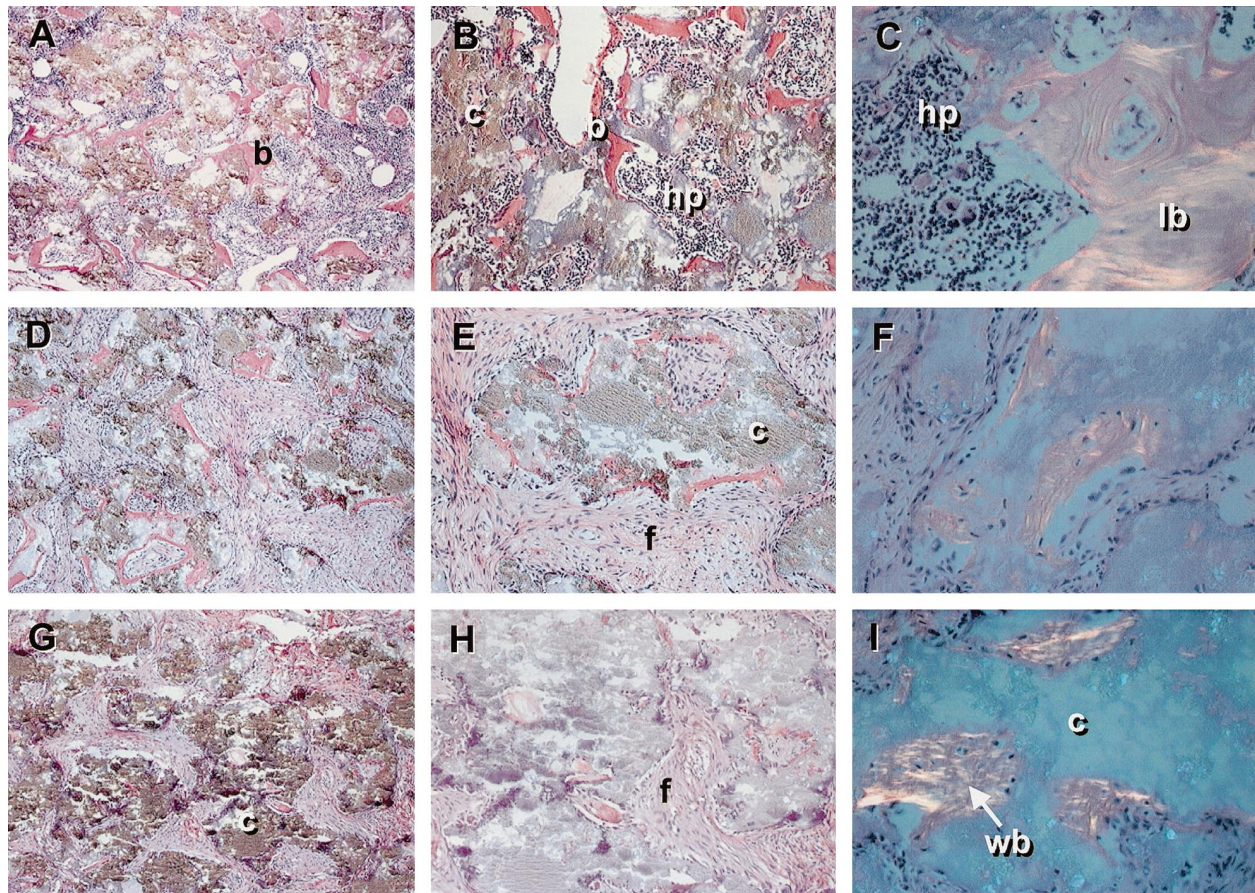


FIG. 4. Transplantation of populations of FD stromal cells into immunocompromised mice regenerates FD. (A–C) Transplant of a control strain of normal marrow stromal cells. Note abundant bone and complete hematopoiesis (megakaryocytes are shown in C). (D–F) Transplants of multicolony-derived strains of stromal cells grown from patient 2. (G–I) Transplants of multicolony-derived strains of stromal cells grown from patient 3. Bone formation is scant, abundant fibrous tissue develops en lieu of hematopoiesis, and there is no adipogenesis. As indicated by collagen orientation revealed by polarized light microscopy, bone that forms is woven in structure throughout (compare F and I with C). A, B, D, and E transmitted light; C, F, and I polarized light. H&E staining, demineralized paraffin sections. c, carrier; b, bone; lb, lamellar bone; wb, woven bone; f, fibrous tissue; hp, hematopoiesis.

or polyostotic) that match the known occurrence of the same type of mutations in isolated endocrine lesions^(8–11) and even in isolated skin lesions.⁽²⁶⁾ We deliberately omitted from the present series mutation-positive patients who may have had an incomplete MAS but feature more than one system involvement (e.g., monostotic FD and one skin lesion, or monostotic FD and acromegaly but no skin lesions). Taken together, these data strongly indicate that a continuous spectrum of phenotypic expression links different clinical presentations of the same underlying genetic disorder.

Therefore, recognition of the presence of activating *GNAS1* mutations, not only the relatively rare MAS, in all 8 FD patients is important because it highlights a common pathogenetic mechanism and a common therapeutic approach. Although uncontrolled studies have suggested that bisphosphonates may be beneficial in FD patients,^(27,28) an effective treatment for FD has not yet been developed. Hopefully, new treatments will be proposed based on more detailed knowledge of pathophysiological consequences of

GNAS1 mutations and *Gsα* overactivity in cells found in the bone environment. We previously identified peculiar changes, putatively reflecting excess generation of cAMP, in osteogenic cells in MAS-associated FD.^(19,22) The same changes occur equally, as shown here, in the non-MAS variants of the disease. Furthermore, we have shown here that using an *in vivo* transplantation assay, MAS⁽¹⁸⁾ and non-MAS FD-derived stromal cells behave in a comparable fashion. Under the same conditions, normal stromal cells form a complete ectopic ossicle made up of predominantly lamellar bone, hematopoietic marrow, and adipocytes.^(20,21) In contrast, FD-derived cells fail to establish a hematopoiesis-supporting stroma, including adipocytes, and form less structurally sound and/or less abundant bone. These findings further emphasize the link between stromal cell dysfunction and the underlying mutation in both MAS and non-MAS FD tissues.

The high prevalence of *GNAS1* mutation in non-MAS FD patients suggests that mutations of the *GNAS1* gene should be included in the clinical/pathological evaluation of FD

patients. In this context, the development of methods for mutation analysis that are reliable, sensitive, and convenient certainly is desirable. The detection of rare somatic mutations within a population of normal cells has engendered numerous approaches. Cloning the cells to near purity allows one to sufficiently enrich the mutant allele's contribution to the genomic DNA to allow assignment of the mutation from direct sequencing of PCR-amplified DNA.

Several other methods have been published to determine the presence of the mutations in a mixed cell population. Shenker et al.⁽³⁾ have shown that the presence of the mutations could be detected by specific oligo-binding to PCR products, and Candelieri et al.⁽²⁹⁾ could detect mutations by using four rounds of tandem PCR amplification and endonuclease digestions followed by sequencing. In the present report, we show that suppression of the amplification of the wild-type allele by PNA in a single PCR reaction leads to a sequencing reaction that is dominated by the mutant sequence, even when the percentage of mutant cells is low. In fact, direct sequencing of amplified DNA failed to demonstrate mutation in two cases, and mutation could be detected only when amplification of the normal allele was blocked. This approach can likely be tailored to yield results when mutant cells represent 1 cell in 100–1000. (The theoretical limit for 1 µg of genomic DNA as template is ~1 cell in 5000.). If the general hypothesis linking low mutational load to limited, single-site lesion is true, then one would anticipate that a highly sensitive method would be specifically desirable in the analysis of monostotic FD or isolated endocrine lesions.

Finally, it is of interest to note here that analysis of undecalcified sections of native FD lesions reveals obvious osteomalacic changes within the lesional bone. To our knowledge, this is the first histologic demonstration of osteomalacia within the lesional tissue itself. This previously overlooked finding is worth noting for two reasons. First, the additional structural feebleness that osteomalacia conveys to the already structurally compromised lesional bone may reflect on the mode of lesion development, clinical evolution of fracture, and severity of the disease. It is easy to note here that bone deformability, as distinct from fragility, is usually a result of defective bone mineralization and is common in FD and MAS (the "shepherd's crook" deformity of the femur is the best-known example). Second, generalized rachitic radiographic changes as a result of renal phosphate wasting have been noted in a number of MAS FD patients. Along with certain mesenchymal soft tissue tumors and/or hemangiopericytomas, FD is one of the lesions potentially underlying "oncogenic osteomalacia."^(30–32) It implies the local synthesis of a putative and yet-unidentified phosphate-regulating factor, "phosphatonin,"⁽³³⁾ or renal phosphate wasting as a function of Gsα mutation within the kidney.⁽³⁴⁾ Additional study on the occurrence of local or systemic osteomalacia in FD/MAS patients is thus warranted for its potential basic and clinical implications.

In conclusion, by using both standard and novel mutation detection assays, we identified GNAS1 mutations in 8 patients with either craniofacial or axial/appendicular FD that did not exhibit any other feature associated with MAS. Lesional tissue exhibited all of the cardinal histologic

features that are associated with MAS, and populations of stromal cells isolated from these lesions generated fibrous dysplastic ossicles in an in vivo transplantation assay. Furthermore, osteomalacia of the lesional tissue, a factor that may contribute significantly to the development and evolution of skeletal lesions, also was noted. These results indicate that postzygotic mutations of the GNAS1 gene result in a broad range of clinical phenotypes, all of which may benefit from the development of newer therapeutic modalities.

ACKNOWLEDGMENTS

The support of Telethon Fondazione Onlus Grant E.519 (to P.B.) is gratefully acknowledged.

REFERENCES

1. Weinstein LS, Shenker A, Gejman PV, Merino MJ, Friedman E, Spiegel AM 1991 Activating mutations of the stimulatory G protein in the McCune-Albright syndrome. *N Engl J Med* **325**:1688–1695.
2. Schwindinger WF, Francomano CA, Levine MA 1992 Identification of a mutation in the gene encoding the alpha subunit of the stimulatory G protein of adenylyl cyclase in McCune-Albright syndrome. *Proc Natl Acad Sci USA* **89**:5152–5156.
3. Shenker A, Weinstein LS, Sweet DE, Spiegel AM 1994 An activating Gs alpha mutation is present in fibrous dysplasia of bone in the McCune-Albright syndrome. *J Clin Endocrinol Metab* **79**:750–755.
4. Ringel MD, Schwindinger WF, Levine MA 1996 Clinical implications of genetic defects in G proteins. The molecular basis of McCune-Albright syndrome and Albright hereditary osteodystrophy. *Medicine (Baltimore)* **75**:171–184.
5. Spiegel AM 1996 Defects in G protein-coupled signal transduction in human disease. *Annu Rev Physiol* **58**:143–170.
6. Spiegel AM 1997 Inborn errors of signal transduction: Mutations in G proteins and G protein-coupled receptors as a cause of disease. *J Inherit Metab Dis* **20**:113–121.
7. Spiegel AM 1997 The molecular basis of disorders caused by defects in G proteins. *Horm Res* **47**:89–96.
8. Boothroyd CV, Grimmond SM, Cameron DP, Hayward NK 1995 G protein mutations in tumours of the pituitary, parathyroid, and endocrine pancreas. *Biochem Biophys Res Commun* **211**:1063–1070.
9. Boston BA, Mandel S, LaFranchi S, Blizotes M 1994 Activating mutation in the stimulatory guanine nucleotide-binding protein in an infant with Cushing's syndrome and nodular adrenal hyperplasia. *J Clin Endocrinol Metab* **79**:890–893.
10. Derwahl M 1996 Molecular aspects of the pathogenesis of nodular goiters, thyroid nodules and adenomas. *Exp Clin Endocrinol Diabetes* **104 Suppl 4**:32–35.
11. Gorelov VN, Dumon K, Barteneva NS, Palm D, Roher HD, Goretzki PE 1995 Overexpression of Gs alpha subunit in thyroid tumors bearing a mutated Gs alpha gene. *J Cancer Res Clin Oncol* **121**:219–224.
12. Lyons J, Landis CA, Harsh G, Vallar L, Grunewald K, Feichtinger H, Duh QY, Clark OH, Kawasaki E, Bourne HR, McCormick F. 1990 Two G protein oncogenes in human endocrine tumors. *Science* **249**:655–659.
13. Huvo AG 1991 Bone Tumors: Diagnosis, Treatment and Prognosis. Saunders, New York, NY, U.S.A.
14. Alman BA, Greel DA, Wolfe HJ 1996 Activating mutations of Gs protein in monostotic fibrous lesions of bone. *J Orthop Res* **14**:311–315.
15. Marie PJ, de Pollak C, Chanson P, Lomri A 1997 Increased proliferation of osteoblastic cells expressing the activating Gs

- alpha mutation in monostotic and polyostotic fibrous dysplasia. *Am J Pathol* **150**:1059–1069.
16. Lichtenstein L, Jaffe HL 1942 Fibrous dysplasia of bone: A condition affecting one, several or many bones, the graver cases of which may present abnormal pigmentation of skin, premature sexual development, hyperthyroidism, and still other extraskelatal abnormalities. *Arch Pathol* **33**:777–797.
 17. Jaffe HL 1958 Tumors and tumorous conditions of the bones and joints. Lea & Febiger, Philadelphia, PA, U.S.A.
 18. Bianco P, Kuznetsov S, Riminucci M, Fisher LW, Spiegel AM, Gehron Robey P 1998 Reproduction of human fibrous dysplasia of bone in immunocompromised mice by transplanted mosaics of normal and Gs-alpha mutated skeletal progenitor cells. *J Clin Invest* **101**:1737–1744.
 19. Riminucci M, Liu B, Corsi A, Shenker A, Spiegel AM, Gehron Robey P, Bianco P 1999 The histopathology of fibrous dysplasia of bone in patients with activating mutations of the Gs alpha gene: site-specific patterns and recurrent histological hallmarks. *J Pathol* **187**:249–258.
 20. Kuznetsov SA, Krebsbach PH, Satomura K, Kerr J, Riminucci M, Benayahu D, Robey PG 1997 Single-colony derived strains of human marrow stromal fibroblasts form bone after transplantation in vivo. *J Bone Miner Res* **12**:1335–1347.
 21. Krebsbach PH, Kuznetsov SA, Satomura K, Emmons RV, Rowe DW, Gehron Robey P 1997 Bone formation in vivo: Comparison of osteogenesis by transplanted mouse and human marrow stromal fibroblasts. *Transplantation* **63**:1059–1069.
 22. Riminucci M, Fisher LW, Shenker A, Spiegel AM, Bianco P, Gehron Robey P 1997 Fibrous dysplasia of bone in the McCune–Albright syndrome: abnormalities in bone formation. *Am J Pathol* **151**:1587–1600.
 23. Boyde A, Maconnachie E, Reid SA, Delling G, Mundy GR 1986 Scanning electron microscopy in bone pathology: Review of methods, potential, and applications. *Scan Electron Microsc Pt 4*:1537–1554.
 24. Spiegel AM 1996 Mutations in G proteins and G protein-coupled receptors in endocrine disease. *J Clin Endocrinol Metab* **81**:2434–2442.
 25. Happle R 1986 The McCune–Albright syndrome: A lethal gene surviving by mosaicism. *Clin Genetics* **29**:321–324.
 26. Schwartz RA, Spicer MS, Leevy CB, Ticker JB, Lambert WC 1996 Cutaneous fibrous dysplasia: an incomplete form of the McCune–Albright syndrome. *Dermatology* **192**:258–261.
 27. Liens D, Delmas PD, Meunier PJ 1994 Long-term effects of intravenous pamidronate in fibrous dysplasia of bone. *Lancet* **343**:953–954.
 28. Chapurlat RD, Delmas PD, Liens D, Meunier PJ 1997 Long-term effects of intravenous pamidronate in fibrous dysplasia of bone. *J Bone Miner Res* **12**:1746–1752.
 29. Candelieri GA, Roughley PJ, Glorieux FH 1997 Polymerase chain reaction-based technique for the selective enrichment and analysis of mosaic arg201 mutations in G alpha s from patients with fibrous dysplasia of bone. *Bone* **21**:201–206.
 30. Park YK, Unni KK, Beabout JW, Hodgson SF 1994 Oncogenic osteomalacia: A clinicopathologic study of 17 bone lesions. *J Korean Med Sci* **9**:289–298.
 31. Dent CE, Gertner JM 1976 Hypophosphataemic osteomalacia in fibrous dysplasia. *Q J Med* **45**:411–420.
 32. Ryan WG, Nibbe AF, Schwartz TB, Ray RD 1968 Fibrous dysplasia of bone with vitamin D resistant rickets: a case study. *Metabolism* **17**:988–998.
 33. Kumar R 1997 Phosphatonin—a new phosphatoretic hormone? (Lessons from tumour-induced osteomalacia and X-linked hypophosphataemia) (Editorial). *Nephrol Dial Transplant* **12**:11–13.
 34. Zung A, Chalew SA, Schwindinger WF, Levine MA, Phillip M, Jara A, Counts DR, Kowarski AA 1995 Urinary cyclic adenosine 3',5'-monophosphate response in McCune–Albright syndrome: Clinical evidence for altered renal adenylate cyclase activity. *J Clin Endocrinol Metab* **80**:3576–3581.

Address reprint requests to:

*Pamela Gehron Robey
Chief, Craniofacial and Skeletal Diseases Branch
National Institute of Dental and Craniofacial Research
National Institutes of Health
Bethesda, MD 20892, U.S.A.*

Received in original form April 13, 1999; in revised form July 9, 1999; accepted July 21, 1999.